

# Uncertainty-driven Trajectory Truncation for Model-based Offline Reinforcement Learning

Junjie Zhang<sup>1\*</sup>, Jiafei Lyu<sup>1\*</sup>, Xiaoteng Ma<sup>2</sup>, Jiangpeng Yan<sup>3</sup>, Jun Yang<sup>2</sup>, Le Wan<sup>4</sup>, Xiu Li<sup>1†</sup>

<sup>1</sup>Tsinghua Shenzhen International Graduate School, Tsinghua University

<sup>2</sup>Department of Automation, Tsinghua University

<sup>3</sup>Huawei Technology

<sup>4</sup>IEG, Tencent

{zhangjj21, lvjf20}@mails.tsinghua.edu.cn, li.xiu@sz.tsinghua.edu.cn

## Abstract

Equipped with the trained environmental dynamics, model-based offline reinforcement learning (RL) algorithms can often successfully learn good policies from fixed-sized datasets, even some datasets with poor quality. Unfortunately, however, it can not be guaranteed that the generated samples from the trained dynamics model are reliable (e.g., some synthetic samples may lie outside of the support region of the static dataset). To address this issue, we propose Trajectory Truncation with Uncertainty (TATU), which adaptively truncates the synthetic trajectory if the accumulated uncertainty along the trajectory is too large. We theoretically show the performance bound of TATU to justify its benefits. To empirically show the advantages of TATU, we first combine it with two classical model-based offline RL algorithms, MOPO and COMBO. Furthermore, we integrate TATU with several off-the-shelf model-free offline RL algorithms, e.g., BCQ. Experimental results on the D4RL benchmark show that TATU significantly improves their performance, often by a large margin.

## 1 Introduction

Offline reinforcement learning (RL) [Lange *et al.*, 2012] defines the task of learning the optimal policy from a previously gathered fixed-sized dataset by some unknown process. Offline RL eliminates the need for online data collection, which is an advantage over online RL since interacting with the environment can be expensive, or even dangerous, especially in real-world applications. The advances in offline RL raise the opportunity of scaling RL algorithms in domains like autonomous driving [Kiran *et al.*, 2020], healthcare [Riachi *et al.*, 2021], robotics [Gu *et al.*, 2016], etc.

In offline setting, the collected dataset often provides limited coverage in the state-action space. It is therefore hard for the offline agent to well-evaluate out-of-distribution (OOD) state-action pairs, due to the accumulation of extrapolation error [Fujimoto *et al.*, 2018] with bootstrapping. Many model-

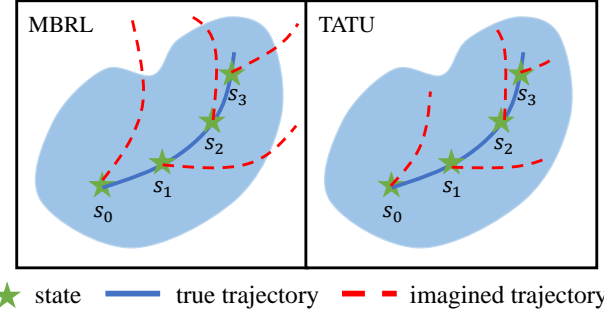


Figure 1: Comparison of TATU against common imagination generation in offline model-based RL (MBRL) methods. TATU truncates the imagined trajectory when the accumulated uncertainty is large and can therefore select good synthetic data in the trajectory. Blue region represents the support region of the static dataset.

free offline RL algorithms have been proposed to avoid OOD actions, such as compelling the learned policy to stay close to the data-collecting policy (behavior policy) [Wu *et al.*, 2019; Kumar *et al.*, 2019; Fujimoto *et al.*, 2018], learning conservative value function [Kumar *et al.*, 2020], leveraging uncertainty quantification [An *et al.*, 2021; Wu *et al.*, 2021], etc. Nevertheless, these methods often suffer from loss of generalization due to limited size of datasets [Wang *et al.*, 2021].

Model-based RL (MBRL) methods, instead, improve the generalization of the agent by generating synthetic imaginations with the learned dynamics model. It has been revealed that directly applying model-based online RL methods like MBPO [Janner *et al.*, 2019] fails on offline datasets [Yu *et al.*, 2020]. Model-based offline RL methods leverage uncertainty quantification [Yu *et al.*, 2020; Kidambi *et al.*, 2020], penalizing value function to enforce conservatism [Yu *et al.*, 2021], planning [Zhan *et al.*, 2022], etc. Utilizing the learned dynamics model for offline data augmentation is also explored recently [Wang *et al.*, 2021; Lyu *et al.*, 2022a]. Nevertheless, there is no guarantee that the generated synthetic samples by the learned model are reliable and lie in the span of the offline dataset. Lyu *et al.* explores a double check mechanism for checking whether the generated samples are reliable, but it requires training bidirectional dynamics models.

In this paper, we propose trajectory truncation with uncertainty (TATU) for reliable imagined trajectory generation.

\*Equal contribution

†Corresponding author

Our key idea is illustrated in Figure 1. As shown, we resort to uncertainty-based methods and truncate the trajectory (i.e., the dynamics model will stop producing imaginations) if the accumulated uncertainty along this trajectory is too large. By doing so, we *enforce conservatism into synthetic data generation* by adaptively clipping the imagined trajectory. TATU can thus ensure that the dynamics model outputs reliable data. Generally, TATU involves three steps: (a) training the environmental dynamics model; (b) constructing an  $\epsilon$ -Pessimistic MDP (see Definition 2); and (c) generating imaginations with the  $\epsilon$ -Pessimistic MDP. We theoretically show that for *any* policy, its performance in the true MDP is lower bounded by the performance in the  $\epsilon$ -Pessimistic MDP, which sheds light on applying TATU in practice.

Intuitively, TATU can be combined with model-based offline RL methods like MOPO [Yu *et al.*, 2020], COMBO [Yu *et al.*, 2021], etc. Moreover, TATU can benefit model-free offline RL methods by training an additional rollout policy and serving trustworthy offline data augmentation.

Our contributions can be summarized below:

- We propose a novel uncertainty-based synthetic trajectory truncation method, TATU, for offline model-based and model-free RL algorithms.
- We theoretically justify the advantages of TATU.
- We combine TATU with two model-based offline RL algorithms, MOPO and COMBO, and observe significant performance improvement upon them.
- We further incorporate TATU with three model-free offline RL algorithms, TD3-BC, CQL, and BCQ. Empirical results show that TATU markedly boosts their performance across a variety of D4RL benchmark tasks.

## 2 Related Work

**Model-free Offline RL.** Recent advances in model-free offline RL generally involve importance sampling [Liu *et al.*, 2019; Nachum *et al.*, 2019], injecting conservatism into value function [Ma *et al.*, 2021; Cheng *et al.*, 2022; Kostrikov *et al.*, 2021b; Kumar *et al.*, 2020; Lyu *et al.*, 2022b], learning latent actions [Zhou *et al.*, 2020; Chen *et al.*, 2022], forcing the learned policy to be close to the behavior policy [Fujimoto and Gu, 2021; Fujimoto *et al.*, 2018; Wu *et al.*, 2019; Kumar *et al.*, 2019; Kostrikov *et al.*, 2021a], adopting uncertainty measurement [An *et al.*, 2021; Wu *et al.*, 2021; Bai *et al.*, 2022], using one-step method [Brandfonbrener *et al.*, 2021], etc. Despite these advances, the generalization capability of the model-free offline RL algorithms is often limited due to the partial coverage of the dataset in the entire state-action space [Wang *et al.*, 2021; Lyu *et al.*, 2022a].

**Model-based Offline RL.** Model-based offline RL methods focus on policy learning under a learned dynamics model. To mitigate extrapolation error [Fujimoto *et al.*, 2018], several methods do not allow the learned policy to visit regions where the discrepancy between the learned dynamics and the true dynamics is large [Argenson and Dulac-Arnold, 2020; Kidambi *et al.*, 2020; Yu *et al.*, 2020; Yang *et al.*, 2022b]. Some researchers seek to constrain the learned policy to be similar to the behavior policy [Cang *et al.*, 2021; Matsushima

*et al.*, 2020; Swazinna *et al.*, 2020]. Also, sequential modeling is explored in offline RL [Chen *et al.*, 2021; Janner *et al.*, 2021]. Some recent advances propose to leverage model-generated synthetic data for better training [Yu *et al.*, 2021; Wang *et al.*, 2021; Lyu *et al.*, 2022a], or to enhance model training [Lu *et al.*, 2021; Lee *et al.*, 2021; Yang *et al.*, 2022a; Rigter *et al.*, 2022; Guo *et al.*, 2022], etc. We, instead, aim at offering higher-quality synthetic data for offline training via an uncertainty-based trajectory truncation method. The most relevant to our work are MOREL [Kidambi *et al.*, 2020], and MOPP [Zhan *et al.*, 2022]. However, our method is different from them. MOREL requires the generated single sample (instead of the trajectory) at each step to lie in a safe region. MOPP leverages offline planning and sorts the *entire* trajectory for high rewarding transitions based on uncertainty after planning is done. TATU, instead, truncates the synthetic trajectory based on the accumulated uncertainty, and adds penalty to the generated samples. TATU *early stops* the imagined trajectory and puts the whole truncated imagined trajectory into the model buffer for policy optimization.

## 3 Background

Reinforcement learning (RL) problem can be formulated by a Markov Decision Process (MDP), which is consisted of  $\mathcal{M} = \langle \mathcal{S}, \mathcal{A}, r, P, \rho_0, \gamma \rangle$ , where  $\mathcal{S}$  denotes the state space,  $\mathcal{A}$  is the action space,  $r(s, a) : \mathcal{S} \times \mathcal{A} \mapsto \mathbb{R}$  is the scalar reward function,  $P(s'|s, a)$  is the transition probability,  $\rho_0(s)$  is the initial state distribution,  $\gamma \in [0, 1)$  is the discount factor. The goal of RL is to find a policy  $\pi(a|s) : s \mapsto \Delta(\mathcal{A})$  such that the expected discounted cumulative long-term rewards with states sampled according to  $\rho_0$  is maximized:

$$\max_{\pi} J_{\rho_0}(\pi, \mathcal{M}) := \mathbb{E}_{s \sim \rho_0, \pi} \left[ \sum_{t=0}^{\infty} \gamma^t r(s_t, a_t) \middle| s_0 = s \right], \quad (1)$$

where  $\Delta(\cdot)$  denotes the probability simplex. We further denote the optimal policy  $\pi^* := \arg \max_{\pi} J_{\rho_0}(\pi, \mathcal{M})$ .

In offline RL, the agent can not interact with the environment, and can only get access to a previously logged dataset  $\mathcal{D}_{\text{env}} = \{(s, a, r, s')\}$ . The data can be collected by one or a mixture of behavior policy  $\mu$ , which are often unknown. Offline RL aims at learning the optimal batch-constraint policy. Model-based offline RL methods learn the environmental dynamics model  $\hat{P}(\cdot|s, a)$  solely from the dataset, and leverage the learned model to optimize the policy. Typically, the transition probability model  $\hat{P}(\cdot|s, a)$  is trained using maximum likelihood estimation. A reward function  $\hat{r}(s, a)$  can also be learned if it is unknown. We assume the reward function is known in this work. Then we can construct a model MDP  $\hat{\mathcal{M}} = \langle \mathcal{S}, \mathcal{A}, \hat{r}, \hat{P}, \hat{\rho}_0, \gamma \rangle$ . During training, the synthetic samples generated by the learned dynamics model will be put into the model buffer  $\mathcal{D}_{\text{model}}$  and the policy is finally updated using data sampled from  $\mathcal{D}_{\text{env}} \cup \mathcal{D}_{\text{model}}$ .

## 4 Trajectory Truncation with Uncertainty

In this section, we first provide some theoretical insights of our proposed trajectory truncation with uncertainty (TATU). Then, we present the detailed practical algorithm for TATU.

## 4.1 Theoretical Analysis

To determine whether the generated synthetic trajectory is reliable, we define the accumulated uncertainty along the trajectory (AUT) and truncation indicator below.

**Definition 1.** Given a state-action sequence  $\{s_i, a_i\}_{i=0}^h$ , define accumulated uncertainty along the trajectory at step  $t$  as:

$$U_t(s_t, a_t) = \sum_{i=0}^t \gamma^i D_{\text{TV}}(\hat{P}(\cdot|s_i, a_i), P(\cdot|s_i, a_i)). \quad (2)$$

Furthermore, we define the truncation indicator as:

$$T_t^\epsilon(s, a) = \begin{cases} 0, & \text{if } U_t(s_t, a_t) \leq \epsilon, \\ 1, & \text{otherwise,} \end{cases} \quad (3)$$

where  $\hat{P}(\cdot|s, a)$  is the trained environmental transition probability,  $P(\cdot|s, a)$  is the true dynamics, and  $D_{\text{TV}}(p, q)$  is the total variation distance between two distributions  $p, q$ . Intuitively,  $U_t(s, a)$  measures how much uncertainty is accumulated along the imagined trajectory and  $T_t^\epsilon(s, a)$  illustrates whether the trajectory ought to be truncated or not. If the accumulated uncertainty is too large (e.g., exceeds the threshold  $\epsilon$ ), then the synthetic trajectory will be truncated and no more forward imagination will be included in the model buffer. We denote  $u(s, a) = D_{\text{TV}}(\hat{P}(\cdot|s, a), P(\cdot|s, a))$  as the uncertainty measurement for state-action pair  $(s, a)$ . It is easy to find that  $\text{AUT } U_t(s_t, a_t) = \sum_{i=0}^t \gamma^i u(s_i, a_i)$ . It is easy to see that this uncertainty measurement is bounded by  $u_{\max}$  almost surely, i.e.,  $|u(s, a)| \leq u_{\max} \leq 1 < \infty, \forall s, a$ .

We further define the  $\epsilon$ -pessimistic MDP as follows:

**Definition 2** ( $\epsilon$ -Pessimistic MDP). The  $\epsilon$ -Pessimistic MDP is defined by the tuple  $\hat{\mathcal{M}}_p = \langle \mathcal{S}, \mathcal{A}, r_p, \hat{P}_p, \hat{\rho}_0, \gamma \rangle$ , where  $\mathcal{S}, \mathcal{A}$  are state space and action space in the actual MDP  $\mathcal{M}$ ,  $\hat{\rho}_0$  is the initial state distribution learned from the dataset  $\mathcal{D}$ . The transition dynamics and reward function for  $\hat{\mathcal{M}}_p$  gives:

$$\hat{P}_p(\cdot|s_t, a_t) = \begin{cases} 0, & \text{if } T_t^\epsilon(s_t, a_t) = 1, \\ \hat{P}(\cdot|s_t, a_t), & \text{otherwise,} \end{cases} \quad (4)$$

$$r_p(s_t, a_t) = \begin{cases} r(s_t, a_t) - \lambda u(s_t, a_t) - \kappa, & \text{if } T_t^\epsilon(s_t, a_t) = 1, \\ r(s_t, a_t) - \lambda u(s_t, a_t), & \text{otherwise,} \end{cases} \quad (5)$$

where  $\kappa$  is the penalty for truncation state, and  $\lambda$  is the uncertainty penalty coefficient for each state-action pair  $(s, a)$ . By introducing the  $\epsilon$ -Pessimistic MDP formulation, we involve conservatism into the reward function and the imagined state-action sequence. The trajectory imagination will be terminated if the truncation indicator  $T_t^\epsilon = 1$  i.e., the accumulated uncertainty  $U_t(s_t, a_t)$  exceeds  $\epsilon$  at horizon  $t$ . An additional reward penalty  $\kappa$  will be allocated to the termination state in the synthetic trajectory.

Assume that the reward function is bounded almost surely, i.e.,  $|r(s, a)| \leq r_{\max}, \forall s, a$ . We now derive the performance bound for our  $\epsilon$ -Pessimistic MDP. Due to the space limit, all proofs are omitted and deferred to Appendix A.

**Theorem 1.** Denote  $\bar{r} = r_{\max} + \lambda u_{\max} + \kappa$ . Then the return of any policy  $\pi$  in the  $\epsilon$ -Pessimistic MDP  $\hat{\mathcal{M}}_p$  and its original MDP  $\mathcal{M}$  satisfies:

$$\begin{aligned} J_{\hat{\rho}_0}(\pi, \hat{\mathcal{M}}_p) &\geq J_{\rho_0}(\pi, \mathcal{M}) - \frac{2\bar{r}}{1-\gamma} \cdot D_{\text{TV}}(\rho_0, \hat{\rho}_0) \\ &\quad - \bar{r} \cdot \epsilon - \frac{\bar{r}}{1-\gamma}, \end{aligned} \quad (6)$$

$$J_{\hat{\rho}_0}(\pi, \hat{\mathcal{M}}_p) \leq J_{\rho_0}(\pi, \mathcal{M}) + \frac{2\bar{r}}{1-\gamma} \cdot D_{\text{TV}}(\rho_0, \hat{\rho}_0) + \bar{r} \cdot \epsilon. \quad (7)$$

**Remark:** Our method incurs a tighter performance bound compared to MOrEL. To be specific, our methods guarantees  $|J_{\hat{\rho}_0}(\pi, \hat{\mathcal{M}}_p) - J_{\rho_0}(\pi, \mathcal{M})| \leq \mathcal{O}\left(\frac{r_{\max}}{1-\gamma}\right)$  thanks to the uncertainty-based trajectory truncation. However, MOrEL only ensures that  $|J_{\hat{\rho}_0}(\pi, \hat{\mathcal{M}}_p) - J_{\rho_0}(\pi, \mathcal{M})| \leq \mathcal{O}\left(\frac{r_{\max}}{(1-\gamma)^2}\right)$ .

Theorem 1 indicates that the return difference for any policy  $\pi$  in the true MDP and the  $\epsilon$ -Pessimistic MDP relies on mainly three parts: (1) the total variation distance between the learned and true initial state distribution  $D_{\text{TV}}(\rho_0, \hat{\rho}_0)$ ; (2) the threshold for accumulated uncertainty  $\epsilon$ ; (3) the upper bound for the pessimistic reward function (since  $|r_p| \leq \bar{r}$  almost surely). As an immediate corollary, we have

**Corollary 1.** If the policy in the  $\epsilon$ -Pessimistic MDP is  $\epsilon_\pi$  sub-optimal, i.e.,  $J_{\hat{\rho}_0}(\pi, \hat{\mathcal{M}}_p) \geq J_{\hat{\rho}_0}(\pi^*, \hat{\mathcal{M}}_p) - \epsilon_\pi$ , then we have

$$\begin{aligned} J_{\rho_0}(\pi^*, \mathcal{M}) - J_{\rho_0}(\pi, \mathcal{M}) &\leq \epsilon_\pi + \frac{4\bar{r}}{1-\gamma} \cdot D_{\text{TV}}(\rho_0, \hat{\rho}_0) \\ &\quad + 2\bar{r}\epsilon + \frac{\bar{r}}{1-\gamma}. \end{aligned}$$

This corollary illustrates the sub-optimality  $(J(\pi^*, \mathcal{M}) - J(\pi, \mathcal{M}))$  of the policy trained with the  $\epsilon$ -Pessimistic MDP. If the dataset covers all possible transitions, i.e., the dataset is large enough, then it is easy to find both  $D_{\text{TV}}(\rho_0, \hat{\rho}_0)$  and  $\epsilon$  approach 0 since the imagined samples will lie in the support region of the dataset with high probability. Naturally, the above upper bound can be further simplified.

**Corollary 2.** If the dataset is large enough, then we have

$$J_{\rho_0}(\pi^*, \mathcal{M}) - J_{\rho_0}(\pi, \mathcal{M}) \leq \epsilon_\pi + \frac{\bar{r}}{1-\gamma}.$$

We then present the algorithmic details for TATU below.

## 4.2 Practical Algorithm

The practical implementation of TATU can be generally divided into three steps:

**Training Dynamics Models:** Following prior work [Janner *et al.*, 2019], we train the dynamics model  $\hat{P}(\cdot|s, a)$  with a neural network  $\hat{p}_\psi(s'|s, a)$  parameterized by  $\psi$  that produces a Gaussian distribution over the next state, i.e.,  $\hat{p}_\psi(s'|s, a) = \mathcal{N}(\mu_\theta(s, a), \Sigma_\phi(s, a))$ ,  $\psi = \{\theta, \phi\}$ . We train an ensemble of  $N$  dynamics models  $\{\hat{p}_\psi^i = \mathcal{N}(\mu_\theta^i, \Sigma_\phi^i)\}_{i=1}^N$ . We denote the loss function for training the forward dynamics model as  $\mathcal{L}_\psi$ .

Then each model in the ensemble is trained independently via maximum log-likelihood:

$$\mathcal{L}_\psi = \mathbb{E}_{(s, a, r, s') \sim \mathcal{D}} [-\log \hat{p}_\psi(s'|s, a)]. \quad (8)$$

We model the difference in the current state and next state, i.e.,  $\mu_\theta(s, a) = s + \delta_\theta(s, a)$  to ensure local continuity.

**Constructing  $\epsilon$ -Pessimistic MDP:** After the environmental dynamics model is well-trained, we can utilize it to construct the  $\epsilon$ -Pessimistic MDP by following Equation (4) and (5) in Definition 2. It is then important to decide which uncertainty measurement to use in practice (as true transition probability  $P(s'|s, a)$  is often unknown), and how to decide the uncertainty threshold  $\epsilon$ . As a valid and reasonable uncertainty measurement, we require  $u(s, a)$  can capture how uncertain the state-action pair  $(s, a)$  is, and satisfy  $|u(s, a)| \leq u_{\max} < \infty$  almost surely for any  $(s, a)$ . MOREL [Kidambi *et al.*, 2020] adopts the ensemble discrepancy as the uncertainty quantifier, i.e.,  $u(s, a) = \max_{i,j} \|\mu_\theta^i(s, a) - \mu_\theta^j(s, a)\|_2$ , where  $\|\cdot\|_2$  is the L2-norm and  $\mu_\theta^i(s, a), \mu_\theta^j(s, a), i, j \in \{1, \dots, N\}$  are mean vectors of the Gaussian distributions in the ensemble. MOPO [Yu *et al.*, 2020] utilizes the maximum standard deviation of the learned models in the ensemble as the uncertainty estimator, i.e.,  $u(s, a) = \max_{i=1}^N \|\Sigma_\phi^i(s, a)\|_F$ , where

$\|\cdot\|_F$  is the Frobenius-norm.  $\|\mathbf{A}\|_F = \sqrt{\sum_{i=1}^m \sum_{j=1}^n |a_{ij}|}$  for matrix  $\mathbf{A}$  with size  $m \times n$ . Empirically, we do not observe much performance difference with these quantifiers in our experiments. We then use an MOPO-style uncertainty estimator in this work. Such uncertainty measurement generally reveals whether the state-action pair is reliable, and satisfies  $|u(s, a)| \leq u_{\max} < \infty$ . One can also enforce this by clipping  $u(s, a)$  to  $[-u_{\max}, u_{\max}]$  with a manually set upper bound.

As for the uncertainty threshold  $\epsilon$ , one naïve way is to set a constant threshold. However, this often lacks flexibility and the best threshold may be quite varied for different datasets. We instead propose to measure the uncertainty on *all of the samples* in the dataset  $\mathcal{D}$ . We then take the maximum transition uncertainty in the dataset and set the uncertainty threshold based on:

$$\epsilon = \frac{1}{\alpha} \max_{i \in [\mathcal{D}]} u(s_i, a_i) = \frac{1}{\alpha} \max_{i \in [\mathcal{D}]} \max_{j \in [N]} \|\Sigma_\phi^j(s_i, a_i)\|_F, \quad (9)$$

where  $[k] = \{1, \dots, k\}$ ,  $(s_i, a_i) \sim \mathcal{D}$ ,  $i \in [\mathcal{D}]$ , and  $\alpha \in \mathbb{R}_+$  is the key hyperparameter that controls the strength of the threshold. By using a larger  $\alpha$ , TATU becomes more conservative and includes fewer imagined samples into the model buffer  $\mathcal{D}_{\text{model}}$ . While if a small  $\alpha$  is used, TATU exhibits more tolerance to generated data. The total uncertainty is controlled by the maximum uncertainty in the real dataset (i.e.,  $\max_{i=1}^{|\mathcal{D}|} u(s_i, a_i)$ ), which usually varies with different datasets. This allows a flexible and reasonable uncertainty threshold for adaptively selecting good imaginations.

**Conservative Trajectory Generation:** Once the uncertainty threshold  $\epsilon$  is ready, we can generate conservative trajectories. We first sample starting state  $s_0$  from the static dataset  $\mathcal{D}$  and generate an imagined trajectory  $\hat{\tau} = \{\hat{s}_j, a_j, r_j, \hat{s}_{j+1}\}_{j=0}^{h-1}$  with the learned dynamics  $\hat{p}_\psi$ , where  $h$  is the horizon length. We simultaneously calculate the accumulated uncertainty of

---

**Algorithm 1** Trajectory Truncation with Uncertainty (TATU)

---

```

1: Require: Offline dataset  $\mathcal{D}$ , iteration  $N_1$ , horizon  $h$ , reward penalty coefficient  $\lambda$ , termination penalty  $\kappa$ 
2: Initialize model buffer  $\mathcal{D}_{\text{model}} \leftarrow \emptyset$ 
3: Train the ensemble dynamics models  $\{\hat{p}_\psi^i(s'|s, a) = \mathcal{N}(\mu_\theta^i(s, a), \Sigma_\phi^i(s, a))\}_{i=1}^N$  on  $\mathcal{D}$  using Equation (8)
4: Calculate the truncation threshold  $\epsilon$  using Equation (9)
5: (Optional) Train a rollout policy via Equation (10)
6: for epoch in 1 to  $N_1$  do
7:   Sample state  $s_0$  from dataset  $\mathcal{D}$ 
8:   for  $j$  in 1 to  $h$  do
9:     Sample an action  $a_j \sim \pi(\cdot|s_j)$  // learned policy
10:    (Optional) Draw an action  $a_j$  from the rollout policy

11:   Randomly pick dynamics  $\hat{p}$  from  $\{\hat{p}_\psi^i\}_{i=1}^N$  and sample next state  $s_{j+1} \sim \hat{p}$ 
12:   Calculate reward according to Equation (5)
13:   Calculate accumulated uncertainty along the trajectory  $U_j = \sum_{k=1}^j \left[ \max_{i=1}^N \|\Sigma_\phi^i(s_k, a_k)\|_F \right]$ 
14:   if  $U_j \leq \epsilon$  then
15:     Put the imagined transition  $(s_j, a_j, r_j, s_{j+1})$  into the model buffer  $\mathcal{D}_{\text{model}}$ 
16:   else
17:     break // Truncate the synthetic trajectory
18:   end if
19: end for
20: Sample data from  $\mathcal{D} \cup \mathcal{D}_{\text{model}}$  and use the base algorithm (e.g., SAC, CQL, BCQ) to optimize policy  $\pi$ 
21: end for

```

---

the imagined trajectory  $U_t(s_t, a_t)$  at horizon  $t$ ,  $t \in [1, h]$ . The generated trajectory is truncated at horizon  $t$  if  $U_t(s_t, a_t) > \epsilon$ . In deep RL, we usually sample a mini-batch of data from the real dataset  $\mathcal{D}$  of size  $B$  with bootstrapping. By leveraging the learned dynamics model, we then can get  $B$  imagined trajectories, provably with different lengths (as the accumulated uncertainty varies with different starting states). We can incorporate TATU with existing popular model-based offline RL algorithms such as MOPO [Yu *et al.*, 2020], COMBO [Yu *et al.*, 2021], etc. Here, the actions in the imagined trajectory are generated with the learned policy  $\pi$ .

TATU can also be incorporated with off-the-shelf model-free offline RL methods, where TATU serves as a role of offline data augmentation to improve the generalization ability of model-free offline RL algorithms. At this time, we need to train an additional rollout policy such that the data augmentation process is isolated from the policy optimization process, i.e., the dataset is augmented beforehand. To avoid potential OOD actions, we model the rollout policy using the conditional variational auto-encoder (CVAE) [Kingma and Welling, 2013]. We choose CVAE as it guarantees that the generated actions lie in the span of the dataset<sup>1</sup>. The CVAE is made up of an encoder  $E_\xi(s, a)$  that produces a latent variable  $z$  under the Gaussian distribution and a decoder  $D_\nu(s, z)$

<sup>1</sup>One can also use other generative models like GAN [Mirza and Osindero, 2014], diffusion model [Ho *et al.*, 2020], etc.

Table 1: Normalized average score comparison of TATU+MOPO and TATU+COMBO against their base algorithms and some recent baselines on the D4RL MuJoCo “-v2” dataset. half = halfcheetah, r = random, m = medium, m-r = medium-replay, m-e = medium-expert. Each algorithm is run for 1M gradient steps with 5 different random seeds. We report the final performance.  $\pm$  captures the standard deviation. We bold the top 2 score of the left part and the best score of the right part.

Task Name	TATU+MOPO	MOPO	TATU+COMBO	COMBO	BC	CQL	IQL	DT	MOReL
half-r	$33.3 \pm 2.6$	<b>35.9</b>	$29.3 \pm 2.7$	<b>38.8</b>	2.2	17.5	13.1	-	<b>38.9</b>
hopper-r	<b>31.3</b> $\pm 0.6$	16.7	<b>31.6</b> $\pm 0.6$	17.9	3.7	7.9	7.9	-	<b>38.1</b>
walker2d-r	<b>10.4</b> $\pm 0.7$	4.2	$5.3 \pm 0.0$	<b>7.0</b>	1.3	5.1	5.4	-	<b>16.0</b>
half-m-r	<b>67.2</b> $\pm 3.3$	<b>69.2</b>	$57.8 \pm 2.7$	55.1	37.6	<b>45.5</b>	44.2	36.6	44.5
hopper-m-r	<b>104.4</b> $\pm 0.9$	32.7	<b>100.7</b> $\pm 1.3$	89.5	16.6	88.7	<b>94.7</b>	82.7	81.8
walker2d-m-r	<b>75.3</b> $\pm 0.2$	73.7	<b>75.3</b> $\pm 1.7$	56.0	20.3	<b>81.8</b>	73.8	66.6	40.8
half-m	$61.9 \pm 2.9$	<b>73.1</b>	<b>69.2</b> $\pm 2.8$	54.2	43.2	47.0	47.4	42.6	<b>60.7</b>
hopper-m	<b>104.3</b> $\pm 1.3$	38.3	<b>100.0</b> $\pm 1.3$	97.2	54.1	53.0	66.2	67.6	<b>84.0</b>
walker2d-m	<b>77.9</b> $\pm 1.6$	41.2	$77.4 \pm 0.9$	<b>81.9</b>	70.9	73.3	<b>78.3</b>	74.0	72.8
half-m-e	$74.1 \pm 1.4$	70.3	<b>96.4</b> $\pm 3.6$	<b>90.0</b>	44.0	75.6	86.7	<b>86.8</b>	80.4
hopper-m-e	<b>107.0</b> $\pm 1.3$	60.6	$106.5 \pm 0.4$	<b>111.1</b>	53.9	105.6	91.5	<b>107.6</b>	105.6
walker2d-m-e	<b>107.9</b> $\pm 0.9$	77.4	<b>114.6</b> $\pm 0.7$	103.3	90.1	107.9	<b>109.6</b>	108.1	107.5
Average score	<b>71.3</b>	49.4	<b>72.0</b>	66.8	36.5	59.1	59.9	-	<b>64.3</b>

that maps  $z$  to the desired space. The objective function for training CVAE is shown below.

$$\mathcal{L}_{\text{CVAE}} = \mathbb{E}_{(s, a, r, s') \sim \mathcal{D}, z \sim E_{\xi}(s', a)} [(a - D_{\nu}(s', z))^2 + D_{\text{KL}}(E_{\xi}(s', a) \parallel \mathcal{N}(0, \mathbf{I}))], \quad (10)$$

where the encoder  $E_{\xi}(s, a)$  and decoder  $D_{\nu}(s, z)$  are parameterized by  $\xi, \nu$ , respectively.  $D_{\text{KL}}(p \parallel q)$  denotes the KL-divergence between two distributions  $p, q$ , and  $\mathbf{I}$  is an identity matrix. When drawing an action from the rollout policy, we first sample a latent variable  $z$  from the multivariate Gaussian distribution  $\mathcal{N}(0, \mathbf{I})$  and process it along with the current state  $s$  with the decoder  $D_{\nu}(s, z)$  to get the resulting action.

We summarize the detailed pseudo code for TATU in Algorithm 1. Note that when drawing samples from  $\mathcal{D} \cup \mathcal{D}_{\text{model}}$ , we sample a proportion of  $\eta B$  real data from real dataset  $\mathcal{D}$  and a proportion of  $(1-\eta)B$  synthetic data from model buffer  $\mathcal{D}$  given the batch size  $B$  and the real data ratio  $\eta \in [0, 1]$ . We then use the underlying algorithms (e.g., CQL) to optimize the policy. To accommodate the reproducibility, we include our source code in the supplementary material.

## 5 Experiments

In this section, we empirically examine how much can TATU benefit existing offline RL methods. Throughout our experimental evaluation, we aim at answering the following questions: (1) How much performance gain can model-based offline RL methods acquire when combined with TATU? (2) Can TATU also benefit model-free offline RL algorithms?

To answer these questions, we first combine TATU with two popular model-based offline RL algorithms, MOPO [Yu *et al.*, 2020] and COMBO [Yu *et al.*, 2021] to examine whether TATU can boost their performance in Section 5.1. We also integrate TATU with three off-the-shelf model-free offline RL methods including CQL [Kumar *et al.*, 2020], TD3\_BC [Fujimoto and Gu, 2021], and BCQ [Fujimoto *et al.*, 2021].

, 2018], to see whether TATU can also benefit them in Section 5.2. We conduct experiments on D4RL [Fu *et al.*, 2020] MuJoCo datasets for evaluation. In Section 5.3, We provide a detailed parameter study on some important hyperparameters in TATU, e.g., rollout horizon. We further compare TATU against other data selection methods in Section 5.4.

### 5.1 Combination with Model-based Offline RL

Since TATU is designed intrinsically for reliable imagination generation in a model-based scenario, we incorporate it with two widely used offline model-based RL algorithms, MOPO [Yu *et al.*, 2020] and COMBO [Yu *et al.*, 2021], giving rise to TATU+MOPO and TATU+COMBO. Since MOPO already penalizes the reward signal with uncertainty, we only add an additional penalty  $\kappa$  to the termination state. TATU modifies the way of imagination generation and concretely rejects bad transition tuples in these methods.

To examine whether TATU can achieve performance improvement upon MOPO and COMBO, we conduct experiments on 12 D4RL [Fu *et al.*, 2020] MuJoCo datasets, which includes three tasks: *halfcheetah*, *hopper*, *walker2d*. We adopt four types of datasets for each task: *random*, *medium*, *medium-replay*, and *medium-expert*, as they are typically utilized for performance evaluation in model-based offline RL. We compare TATU+MOPO, TATU+COMBO against their base algorithms. We also compare them against some common baselines in offline RL, such as behavior cloning (BC), IQL [Kostrikov *et al.*, 2021a], Decision Transformer (DT) [Chen *et al.*, 2021]. We take the results of IQL on medium-level datasets from its original paper and run with its official implementation<sup>2</sup> on random and expert datasets. The results of BC are acquired by our own implementation. For methods that were originally evaluated on “-v0” datasets, we retrain them with the official implementations on “-v2” datasets, and take the results of other baselines from their original papers.

<sup>2</sup>[https://github.com/ikostrikov/implicit\\_q\\_learning](https://github.com/ikostrikov/implicit_q_learning)

Table 2: Normalized average score comparison of TATU+TD3\\_BC, TATU+CQL and TATU+BCQ against their base algorithms and some recent baselines on the D4RL MuJoCo “-v2” dataset. half = halfcheetah, r = random, m = medium, m-r = medium-replay, m-e = medium-expert, e = expert. Each algorithm is run for 1M gradient steps across 5 different random seeds and the final mean performance is reported.  $\pm$  captures the standard deviation. We bold the top 3 score of the left part and the best score of the right part.

Task Name	TATU+TD3\_BC	TD3\_BC	TATU+CQL	CQL	TATU+BCQ	BCQ	BC	IQL	DT
half-r	<b>12.1</b> $\pm$ 2.3	11.0	<b>27.4</b> $\pm$ 2.6	<b>17.5</b>	2.3 $\pm$ 2.3	2.2	2.2	<b>13.1</b>	-
hopper-r	<b>31.6</b> $\pm$ 0.6	8.5	<b>32.3</b> $\pm$ 0.7	7.9	<b>10.3</b> $\pm$ 0.8	7.8	3.7	<b>7.9</b>	-
walker2d-r	<b>21.4</b> $\pm$ 0.0	1.6	<b>23.0</b> $\pm$ 0.0	<b>5.1</b>	3.4 $\pm$ 0.4	4.9	1.3	<b>5.4</b>	-
half-m-r	<b>45.9</b> $\pm$ 0.6	44.6	<b>48.0</b> $\pm$ 0.7	<b>45.5</b>	43.5 $\pm$ 0.3	42.2	37.6	<b>44.2</b>	36.6
hopper-m-r	65.7 $\pm$ 3.9	60.9	<b>96.8</b> $\pm$ 2.6	<b>88.7</b>	<b>72.9</b> $\pm$ 0.4	60.9	16.6	<b>94.7</b>	82.7
walker2d-m-r	<b>81.9</b> $\pm$ 2.7	<b>81.8</b>	<b>85.5</b> $\pm$ 1.2	<b>81.8</b>	77.7 $\pm$ 1.0	57.0	20.3	<b>73.8</b>	66.6
half-m	<b>48.4</b> $\pm$ 2.7	<b>48.3</b>	44.9 $\pm$ 0.3	47.0	<b>47.6</b> $\pm$ 0.2	46.6	43.2	<b>47.4</b>	42.6
hopper-m	<b>62.0</b> $\pm$ 1.0	59.3	<b>68.9</b> $\pm$ 0.9	53.0	<b>71.0</b> $\pm$ 0.3	59.4	54.1	66.2	<b>67.6</b>
walker2d-m	<b>84.3</b> $\pm$ 0.2	<b>83.7</b>	65.7 $\pm$ 0.5	73.3	<b>80.5</b> $\pm$ 0.4	71.8	70.9	<b>78.3</b>	74.0
half-m-e	<b>97.1</b> $\pm$ 3.2	90.7	78.9 $\pm$ 0.5	75.6	<b>96.1</b> $\pm$ 0.2	<b>95.4</b>	44.0	86.7	<b>86.8</b>
hopper-m-e	<b>113.0</b> $\pm$ 1.7	98.0	<b>111.5</b> $\pm$ 1.0	105.6	<b>108.2</b> $\pm$ 0.3	106.9	53.9	91.5	<b>107.6</b>
walker2d-m-e	<b>110.9</b> $\pm$ 0.5	110.1	<b>110.2</b> $\pm$ 0.1	107.9	<b>111.7</b> $\pm$ 0.3	107.7	90.1	<b>109.6</b>	108.1
half-e	<b>97.4</b> $\pm$ 0.4	<b>96.7</b>	90.8 $\pm$ 3.4	<b>96.3</b>	<b>96.3</b> $\pm$ 1.4	89.9	91.8	<b>95.0</b>	-
hopper-e	<b>111.8</b> $\pm$ 1.1	<b>107.8</b>	106.8 $\pm$ 0.9	96.5	103.9 $\pm$ 0.6	<b>109.0</b>	107.7	<b>109.4</b>	-
walker2d-e	<b>110.0</b> $\pm$ 0.1	<b>110.2</b>	108.3 $\pm$ 0.1	108.5	<b>109.7</b> $\pm$ 0.3	106.3	106.7	<b>109.9</b>	-
Average score	<b>72.9</b>	67.5	<b>73.3</b>	67.3	<b>69.0</b>	64.5	49.6	<b>68.9</b>	-

All of the algorithms are run for 1M gradient steps. Table 1 reports the normalized score over the final 10 evaluations for each task and their average performance over 5 different random seeds. It can be found that TATU markedly boosts the performance of both MOPO and COMBO on most of the datasets, often by a large and significant margin. For example, TATU+MOPO achieves a mean score of **104.4** on hopper-medium-replay-v2 and **77.9** on walker2d-medium-v2, while MOPO only attains 32.7 and 41.2 on them, respectively. It is worth noting that MOPO and COMBO gain **44%** and **7.8%** improvement in average score, respectively, with the aid of TATU. We also observe a competitive or better performance of TATU+MOPO and TATU+COMBO on the evaluated datasets against baseline methods like IQL, MORL, etc. TATU+COMBO has the best average score (**72.0**) across all of the datasets, TATU+MOPO achieves an average score of **71.3**. Whereas, the best baseline only achieves 66.8. The empirical evaluations indicate that TATU can significantly benefit the existing model-based offline RL methods.

## 5.2 Combination with Model-free Offline RL

We now demonstrate that TATU can also benefit model-free offline RL algorithms. We first train the dynamics model and an additional CVAE rollout policy. During data generation, we truncate the synthetic trajectory if the accumulated uncertainty along it is large. Importantly, we leverage the rollout policy to produce actions in the imagined trajectory, thus isolating the data augmentation process from the policy optimization process.

To illustrate the generality and effectiveness of TATU, we combine it with three popular model-free offline RL algorithms, CQL [Kumar *et al.*, 2020], BCQ [Fujimoto *et al.*, 2018], and TD3\\_BC [Fujimoto and Gu, 2021], yielding TATU+CQL, TATU+BCQ, and TATU+TD3\\_BC algorithms.

We extensively compare them with their base algorithms and three model-free offline RL baselines (BC, IQL, DT) on 15 D4RL datasets, with additional *expert* datasets of three tasks compared to the experimental evaluation in Section 5.1.

We summarize the experimental results in Table 2. We find that TATU significantly improves the performance of the base algorithms on many datasets, often outperforming them by a remarkable margin, especially on many poor-quality datasets (e.g., random). As an example, TATU+TD3\\_BC has a mean normalized score of **31.6** on hopper-random-v2, while TD3\\_BC itself only achieves 8.5. The three base methods, TD3\\_BC, CQL, BCQ, gains **8.0%**, **8.9%** and **7.0%** performance improvement in average score, respectively. With the conservative and reliable transition generation by our novel synthetic trajectory truncation method, model-free offline RL methods can benefit from better generalization capability, resulting in better performance. Based on these experiments, we conclude that TATU is general and can widely benefit both model-based and model-free offline RL algorithms.

Note that due to space limit, we omit the standard deviation for baseline methods, and the full comparison results of Table 1 and Table 2 can be found in Appendix D.

## 5.3 Parameter Study

There are generally three key hyperparameters in TATU, the rollout horizon  $h$ , the threshold parameter  $\alpha$ , and the real data ratio  $\eta \in [0, 1]$  in a sampled batch from  $\mathcal{D} \cup \mathcal{D}_{\text{model}}$ .

**Rollout horizon  $h$ .** This parameter measures how far that we allow the imagined trajectory to branch. With a larger horizon length for the dynamics model, more diverse data can be included in the model buffer, which, however, also increases the risk of involving bad transitions. This issue can be alleviated by TATU as it adaptively truncates the imagined trajectory. A large horizon length  $h$  can therefore be adopted. To see the

influence of  $h$ , we conduct experiments on hopper-medium-replay-v2 with TATU+MOPO and TATU+TD3.BC. We keep other parameters fixed and sweep  $h$  across  $\{1, 3, 5, 7, 10\}$ . Results in Table 3 indicates that TATU enjoys better performance with a larger horizon and fails with horizon 1. This may be because the diversity of the generated samples is not enough with a too small horizon length. In our experiments, we set the rollout horizon  $h = 5$  by default.

Table 3: Comparison of TATU+MOPO and TATU+TD3.BC with different horizon lengths  $h$  on hopper-medium-replay-v2. The results are run for 1M gradient steps and averaged over the final 10 evaluations and 5 random seeds. Mean performance along with the standard deviation are reported.

horizon $h$	TATU+MOPO	TATU+TD3.BC
1	$26.7 \pm 4.4$	$57.9 \pm 1.9$
3	$100.4 \pm 1.3$	$70.0 \pm 4.9$
5	$104.4 \pm 0.9$	$65.7 \pm 3.9$
7	$102.0 \pm 0.7$	$71.1 \pm 12.4$
10	$103.7 \pm 1.6$	$71.0 \pm 16.8$

**Threshold coefficient  $\alpha$ .** The threshold parameter  $\alpha$  is probably the most critical parameter for TATU, which controls the strength that we reject the generated imaginations (larger  $\alpha$  will reject more transitions). This parameter is highly related to the quality of the dataset, e.g., a large  $\alpha$  is better for expert-level datasets while  $\alpha$  can be small for dataset that is collected by a random policy. Generally, we require  $\alpha \geq 1$ . To show the effects of this parameter, we run TATU+MOPO and TATU+TD3.BC on hopper-medium-replay-v2 with  $\alpha \in \{1.0, 2.0, 3.0, 4.0, 5.0\}$ . We report the experimental results in Table 4. We see that larger  $\alpha$  degrades the agent’s performance of MOPO. This is harmful as the diversity in the imaginations is decreased and a small real data ratio  $\eta$  is adopted in MOPO, while few samples are admitted. For TD3.BC, however, a larger  $\alpha$  is better as small  $\alpha$  enables a large threshold  $\epsilon$ , i.e., bad transitions may be included. We notice that we can luckily find a trade-off of  $\alpha$  for different algorithms.

Table 4: Comparison of TATU+MOPO and TATU+TD3.BC with different threshold coefficient  $\alpha$  on hopper-medium-replay-v2. Each algorithm is run for 1M steps with 5 random seeds. We report the mean performance over the final 10 evaluations, in conjunction with the standard deviation.

Coefficient $\alpha$	TATU+MOPO	TATU+TD3.BC
1.0	$101.4 \pm 0.8$	$32.1 \pm 11.1$
2.0	$104.4 \pm 0.9$	$50.2 \pm 4.4$
3.0	$98.7 \pm 3.3$	$52.2 \pm 10.1$
4.0	$96.4 \pm 2.7$	$61.9 \pm 10.7$
5.0	$52.8 \pm 31.7$	$58.6 \pm 13.4$

**Real data ratio  $\eta$ .** The real data ratio controls the proportion of real data in a sampled mini-batch, i.e., it determines how many synthetic samples are used for offline policy learning.  $\eta$  also strongly depends on the specific dataset and setting. Model-based offline RL method usually uses a small  $\eta$ , and the  $\eta$  for model-free offline RL algorithm relies heavily

Table 5: Comparison of TATU+MOPO and TATU+TD3.BC under different real data ratio  $\eta$  on hopper-medium-replay-v2. The results are averaged over the final 10 evaluations and 5 random seeds. We report the mean performance and the standard deviation.

Real data ratio $\eta$	TATU+MOPO	TATU+TD3.BC
0.05	$104.4 \pm 0.9$	$9.1 \pm 4.4$
0.25	$101.5 \pm 3.8$	$39.7 \pm 15.6$
0.5	$101.1 \pm 2.7$	$65.4 \pm 1.2$
0.7	$92.9 \pm 2.9$	$65.7 \pm 3.9$
0.9	$85.1 \pm 12.4$	$68.8 \pm 17.9$

on the quality of the dataset, e.g., a small  $\eta$  is preferred for datasets with poor quality, and a larger  $\eta$  is better for expert datasets. To see how  $\eta$  affects the performance of model-based and model-free offline RL algorithms with TATU, we run TATU+MOPO and TATU+TD3.BC with different real data ratio  $\eta \in \{0.05, 0.25, 0.5, 0.7, 0.9\}$  on hopper-medium-replay-v2. We summarize the results in Table 5, where we find that TATU+MOPO achieves very good performance under a wide range of  $\eta$ , even a large  $\eta = 0.9$  thanks to the conservative trajectory truncation by TATU. As the dataset is of medium quality, TATU+TD3.BC attains higher performance with larger  $\eta$ , as expected.

#### 5.4 Comparison with Other Relevant Methods

In order to further show the advantages of our proposed TATU method, we compare it against other data selection methods, including CABI [Lyu *et al.*, 2022a] and MOPP [Zhan *et al.*, 2022]. MOPP selects transitions by performing planning and then sorting the trajectory such that each sample in the left trajectory meets the uncertainty constraint. CABI trains bidirectional dynamics models and only admits transitions that the forward and backward model agree on. TATU ensures reliable data generation via adaptively truncating the imagined trajectory. We combine TATU and CABI with TD3.BC and conduct experiments on 6 *random, medium-expert* datasets from D4RL MuJoCo datasets. We follow the guidance in the CABI paper and implement it on our own. We take the results of MOPP from its original paper directly. The results are presented in Table 6. We find that TATU+TD3.BC outperforms MOPP and CABI on most of the datasets, achieving the best performance on 4 out of 6 datasets. Furthermore, we also observe remarkable advantages of TATU on top of some base algorithms, e.g., CQL, COMBO, over MOPP (see experimental results in Table 1, 2, and 6). These we believe can well illustrate the superiority of TATU.

Table 6: Comparison of TATU against CABI (with TD3.BC as the base algorithm) and MOPP on six datasets from D4RL.

Task Name	TATU+TD3.BC	CABI+TD3.BC	MOPP
half-r	$12.1 \pm 2.3$	$14.3 \pm 0.4$	$9.4 \pm 2.6$
hopper-r	<b><math>31.6 \pm 0.6</math></b>	$15.7 \pm 11.1$	$13.7 \pm 2.5$
walker-r	<b><math>21.4 \pm 0.0</math></b>	$6.0 \pm 0.3$	$6.3 \pm 0.1$
half-m-e	$97.1 \pm 3.2$	$94.8 \pm 1.0$	<b><math>106.2 \pm 5.1</math></b>
hopper-m-e	<b><math>113.0 \pm 1.7</math></b>	$111.4 \pm 0.3$	$95.4 \pm 28.0$
walker2d-m-e	<b><math>110.9 \pm 0.5</math></b>	$110.5 \pm 0.6$	$92.9 \pm 14.1$

## 6 Conclusion

In this paper, we propose trajectory truncation with uncertainty (TATU) to facilitate both model-based and model-free offline RL algorithms. We adaptively truncate the imagined trajectory if the accumulated uncertainty of this trajectory is too large, which ensures the reliability of the synthetic samples. We theoretically demonstrate the advantages of our proposed truncation method. Empirical results on the D4RL benchmark show that TATU markedly improves the performance of model-based offline RL methods (e.g., MOPO) and model-free offline RL methods (e.g., CQL). These altogether illustrate the generality and effectiveness of TATU.

## References

[An *et al.*, 2021] Gaon An, Seungyong Moon, Jang-Hyun Kim, and Hyun Oh Song. Uncertainty-based offline reinforcement learning with diversified q-ensemble. In *Neural Information Processing Systems*, 2021.

[Argenson and Dulac-Arnold, 2020] Arthur Argenson and Gabriel Dulac-Arnold. Model-based offline planning. In *International Conference on Learning Representations*, 2020.

[Bai *et al.*, 2022] Chenjia Bai, Lingxiao Wang, Zhuoran Yang, Zhihong Deng, Animesh Garg, Peng Liu, and Zhao-ran Wang. Pessimistic bootstrapping for uncertainty-driven offline reinforcement learning. In *International Conference on Learning Representation*, 2022.

[Brandfonbrener *et al.*, 2021] David Brandfonbrener, William F. Whitney, Rajesh Ranganath, and Joan Bruna. Offline rl without off-policy evaluation. In *Neural Information Processing Systems*, 2021.

[Cang *et al.*, 2021] Catherine Cang, Aravind Rajeswaran, P. Abbeel, and Michael Laskin. Behavioral priors and dynamics models: Improving performance and domain transfer in offline rl. *ArXiv*, abs/2106.09119, 2021.

[Chen *et al.*, 2021] Lili Chen, Kevin Lu, Aravind Rajeswaran, Kimin Lee, Aditya Grover, Michael Laskin, P. Abbeel, A. Srinivas, and Igor Mordatch. Decision transformer: Reinforcement learning via sequence modeling. In *Neural Information Processing Systems*, 2021.

[Chen *et al.*, 2022] Xi Chen, Ali Ghadirzadeh, Tianhe Yu, Jianhao Wang, Yuan Gao, Wenzhe Li, Liang Bin, Chelsea Finn, and Chongjie Zhang. LAPO: Latent-variable advantage-weighted policy optimization for offline reinforcement learning. In *Advances in Neural Information Processing Systems*, 2022.

[Cheng *et al.*, 2022] Ching-An Cheng, Tengyang Xie, Nan Jiang, and Alekh Agarwal. Adversarially trained actor critic for offline reinforcement learning. In *International Conference on Machine Learning*, 2022.

[Fu *et al.*, 2020] Justin Fu, Aviral Kumar, Ofir Nachum, G. Tucker, and Sergey Levine. D4rl: Datasets for deep data-driven reinforcement learning. *ArXiv*, abs/2004.07219, 2020.

[Fujimoto and Gu, 2021] Scott Fujimoto and Shixiang Gu. A minimalist approach to offline reinforcement learning. In *Advances in Neural Information Processing Systems*, 2021.

[Fujimoto *et al.*, 2018] Scott Fujimoto, David Meger, and Doina Precup. Off-policy deep reinforcement learning without exploration. In *International Conference on Machine Learning*, 2018.

[Gu *et al.*, 2016] Shixiang Shane Gu, Ethan Holly, Timothy P. Lillicrap, and Sergey Levine. Deep reinforcement learning for robotic manipulation with asynchronous off-policy updates. *2017 IEEE International Conference on Robotics and Automation (ICRA)*, pages 3389–3396, 2016.

[Guo *et al.*, 2022] Kaiyang Guo, Yunfeng Shao, and Yanhui Geng. Model-based offline reinforcement learning with pessimism-modulated dynamics belief. In *Neural Information Processing Systems*, 2022.

[Ho *et al.*, 2020] Jonathan Ho, Ajay Jain, and P. Abbeel. Denoising diffusion probabilistic models. In *Neural Information Processing Systems*, 2020.

[Janner *et al.*, 2019] Michael Janner, Justin Fu, Marvin Zhang, and Sergey Levine. When to trust your model: Model-based policy optimization. In *Neural Information Processing Systems*, 2019.

[Janner *et al.*, 2021] Michael Janner, Qiyang Li, and Sergey Levine. Reinforcement learning as one big sequence modeling problem. In *Neural Information Processing Systems*, 2021.

[Kidambi *et al.*, 2020] Rahul Kidambi, Aravind Rajeswaran, Praneeth Netrapalli, and Thorsten Joachims. Morel : Model-based offline reinforcement learning. In *Neural Information Processing Systems*, 2020.

[Kingma and Welling, 2013] Diederik P. Kingma and Max Welling. Auto-encoding variational bayes. *ArXiv*, abs/1312.6114, 2013.

[Kiran *et al.*, 2020] Bangalore Ravi Kiran, Ibrahim Sobh, Victor Talpaert, Patrick Mannion, Ahmad A. Al Sallab, Senthil Kumar Yogamani, and Patrick P'erez. Deep reinforcement learning for autonomous driving: A survey. *IEEE Transactions on Intelligent Transportation Systems*, 23:4909–4926, 2020.

[Kostrikov *et al.*, 2021a] Ilya Kostrikov, Ashvin Nair, and Sergey Levine. Offline reinforcement learning with implicit q-learning. In *International Conference on Learning Representation*, 2021.

[Kostrikov *et al.*, 2021b] Ilya Kostrikov, Jonathan Tompson, Rob Fergus, and Ofir Nachum. Offline reinforcement learning with fisher divergence critic regularization. In *International Conference on Machine Learning*, 2021.

[Kumar *et al.*, 2019] Aviral Kumar, Justin Fu, G. Tucker, and Sergey Levine. Stabilizing off-policy q-learning via bootstrapping error reduction. In *Neural Information Processing Systems*, 2019.

[Kumar *et al.*, 2020] Aviral Kumar, Aurick Zhou, G. Tucker, and Sergey Levine. Conservative q-learning for offline reinforcement learning. In *Neural Information Processing Systems*, 2020.

[Lange *et al.*, 2012] Sascha Lange, Thomas Gabel, and Martin A. Riedmiller. Batch reinforcement learning. In *Reinforcement Learning*, 2012.

[Lee *et al.*, 2021] Byung-Jun Lee, Jongmin Lee, and Kee-Eung Kim. Representation balancing offline model-based reinforcement learning. In *International Conference on Learning Representations*, 2021.

[Liu *et al.*, 2019] Yao Liu, Adith Swaminathan, Alekh Agarwal, and Emma Brunskill. Off-policy policy gradient with state distribution correction. *ArXiv*, abs/1904.08473, 2019.

[Lu *et al.*, 2021] Cong Lu, Philip J. Ball, Jack Parker-Holder, Michael A. Osborne, and Stephen J. Roberts. Revisiting design choices in model-based offline reinforcement learning. In *International Conference on Learning Representations*, 2021.

[Lyu *et al.*, 2022a] Jiafei Lyu, Xiu Li, and Zongqing Lu. Double check your state before trusting it: Confidence-aware bidirectional offline model-based imagination. In *Neural Information Processing Systems*, 2022.

[Lyu *et al.*, 2022b] Jiafei Lyu, Xiaoteng Ma, Xiu Li, and Zongqing Lu. Mildly conservative q-learning for offline reinforcement learning. In *Neural Information Processing Systems*, 2022.

[Ma *et al.*, 2021] Yecheng Jason Ma, Dinesh Jayaraman, and Osbert Bastani. Conservative offline distributional reinforcement learning. In *Neural Information Processing Systems*, 2021.

[Matsushima *et al.*, 2020] Tatsuya Matsushima, Hiroki Furuta, Yutaka Matsuo, Ofir Nachum, and Shixiang Shane Gu. Deployment-efficient reinforcement learning via model-based offline optimization. In *International Conference on Learning Representations*, 2020.

[Mirza and Osindero, 2014] Mehdi Mirza and Simon Osindero. Conditional generative adversarial nets. In *Neural Information Processing Systems*, 2014.

[Nachum *et al.*, 2019] Ofir Nachum, Bo Dai, Ilya Kostrikov, Yinlam Chow, Lihong Li, and Dale Schuurmans. Algaedice: Policy gradient from arbitrary experience. *ArXiv*, abs/1912.02074, 2019.

[Riachi *et al.*, 2021] Elsa Riachi, Muhammad Mamdani, Michael Fralick, and Frank Rudzicz. Challenges for reinforcement learning in healthcare. *ArXiv*, abs/2103.05612, 2021.

[Rigter *et al.*, 2022] Marc Rigter, Bruno Lacerda, and Nick Hawes. Rambo-rl: Robust adversarial model-based offline reinforcement learning. In *Neural Information Processing Systems*, 2022.

[Swazinna *et al.*, 2020] Phillip Swazinna, Steffen Udluft, and Thomas A. Runkler. Overcoming model bias for robust offline deep reinforcement learning. *Engineering Applications of Artificial Intelligence*, 104, 2020.

[Wang *et al.*, 2021] Jianhao Wang, Wenzhe Li, Haozhe Jiang, Guangxiang Zhu, Siyuan Li, and Chongjie Zhang. Offline reinforcement learning with reverse model-based imagination. In *Neural Information Processing Systems*, 2021.

[Wu *et al.*, 2019] Yifan Wu, G. Tucker, and Ofir Nachum. Behavior regularized offline reinforcement learning. *ArXiv*, abs/1911.11361, 2019.

[Wu *et al.*, 2021] Yue Wu, Shuangfei Zhai, Nitish Srivastava, Joshua M. Susskind, Jian Zhang, Ruslan Salakhutdinov, and Hanlin Goh. Uncertainty weighted actor-critic for offline reinforcement learning. In *International Conference on Machine Learning*, 2021.

[Yang *et al.*, 2022a] Shentao Yang, Shujian Zhang, Yihao Feng, and Mi Zhou. A unified framework for alternating offline model training and policy learning. In *Neural Information Processing Systems*, 2022.

[Yang *et al.*, 2022b] Yijun Yang, Jing Ping Jiang, Tianyi Zhou, Jie Ma, and Yuhui Shi. Pareto policy pool for model-based offline reinforcement learning. In *International Conference on Learning Representations*, 2022.

[Yu *et al.*, 2020] Tianhe Yu, Garrett Thomas, Lantao Yu, Stefano Ermon, James Y. Zou, Sergey Levine, Chelsea Finn, and Tengyu Ma. Mopo: Model-based offline policy optimization. In *Neural Information Processing Systems*, 2020.

[Yu *et al.*, 2021] Tianhe Yu, Aviral Kumar, Rafael Rafailov, Aravind Rajeswaran, Sergey Levine, and Chelsea Finn. Combo: Conservative offline model-based policy optimization. In *Neural Information Processing Systems*, 2021.

[Zhan *et al.*, 2022] Xianyuan Zhan, Xiangyu Zhu, and Haoran Xu. Model-based offline planning with trajectory pruning. In *31st International Joint Conference on Artificial Intelligence and the 25th European Conference on Artificial Intelligence (IJCAI-ECAI 22)*, 2022.

[Zhou *et al.*, 2020] Wenxuan Zhou, Sujay Bajracharya, and David Held. Plas: Latent action space for offline reinforcement learning. In *Conference on Robot Learning*, 2020.

## A Missing Proofs

### A.1 Proof of Theorem 1

In order to show Theorem 1, we first denote the pessimistic MDP  $\mathcal{M}_p$  below:

**Definition 3** (Pessimistic MDP). *The pessimistic MDP is defined by the tuple  $\mathcal{M}_p = \langle \mathcal{S}, \mathcal{A}, r_p, P_p, \rho_0, \gamma \rangle$ , where  $r_p(s, a)$  follows the Equation (5) and  $P_p(\cdot|s, a)$  is given by:*

$$P_p(\cdot|s_t, a_t) = \begin{cases} 0, & \text{if } T_t^\epsilon(s_t, a_t) = 1, \\ P(\cdot|s_t, a_t), & \text{otherwise,} \end{cases} \quad (11)$$

where  $P(\cdot|s, a)$  is the transition probability of the true environmental dynamics.

Then we introduce the following Lemma.

**Lemma 1.** *Set  $\bar{r} = r_{\max} + \lambda u_{\max} + \kappa$ . Given the pessimistic MDP  $\mathcal{M}_p$  and the  $\epsilon$ -Pessimistic MDP  $\hat{\mathcal{M}}_p$ , the return difference of any policy  $\pi$  on the two MDPs is bounded:*

$$\left| J_{\rho_0}(\pi, \mathcal{M}_p) - J_{\hat{\rho}_0}(\pi, \hat{\mathcal{M}}_p) \right| \leq \frac{2\bar{r}}{1-\gamma} D_{\text{TV}}(\rho_0, \hat{\rho}_0) + \bar{r} \cdot \epsilon. \quad (12)$$

*Proof.* By definition, it is easy to find that

$$\begin{aligned} & \left| J_{\rho_0}(\pi, \mathcal{M}_p) - J_{\hat{\rho}_0}(\pi, \hat{\mathcal{M}}_p) \right| \\ &= \left| \mathbb{E}_{\rho_0} \mathbb{E}_{P_p} \left[ \sum_{t=0}^{\infty} \gamma^t r_p(s_t, a_t) \right] - \mathbb{E}_{\hat{\rho}_0} \mathbb{E}_{\hat{P}_p} \left[ \sum_{t=0}^{\infty} \gamma^t r_p(s_t, a_t) \right] \right| \\ &= \left| \mathbb{E}_{\rho_0} \mathbb{E}_{P_p} \left[ \sum_{t=0}^{\infty} \gamma^t r_p(s_t, a_t) \right] - \mathbb{E}_{\hat{\rho}_0} \mathbb{E}_{P_p} \left[ \sum_{t=0}^{\infty} \gamma^t r_p(s_t, a_t) \right] \right. \\ &\quad \left. + \mathbb{E}_{\hat{\rho}_0} \mathbb{E}_{P_p} \left[ \sum_{t=0}^{\infty} \gamma^t r_p(s_t, a_t) \right] - \mathbb{E}_{\hat{\rho}_0} \mathbb{E}_{\hat{P}_p} \left[ \sum_{t=0}^{\infty} \gamma^t r_p(s_t, a_t) \right] \right| \\ &\leq \underbrace{\left| \mathbb{E}_{\rho_0} \mathbb{E}_{P_p} \left[ \sum_{t=0}^{\infty} \gamma^t r_p(s_t, a_t) \right] - \mathbb{E}_{\hat{\rho}_0} \mathbb{E}_{P_p} \left[ \sum_{t=0}^{\infty} \gamma^t r_p(s_t, a_t) \right] \right|}_{L_1} \\ &\quad + \underbrace{\left| \mathbb{E}_{\hat{\rho}_0} \mathbb{E}_{P_p} \left[ \sum_{t=0}^{\infty} \gamma^t r_p(s_t, a_t) \right] - \mathbb{E}_{\hat{\rho}_0} \mathbb{E}_{\hat{P}_p} \left[ \sum_{t=0}^{\infty} \gamma^t r_p(s_t, a_t) \right] \right|}_{L_2}. \end{aligned}$$

It is easy to notice that  $|r_p(s, a)| \leq \bar{r} = r_{\max} + \lambda u_{\max} + \kappa$ . Then for  $L_1$ , we have

$$\begin{aligned} L_1 &= \left| \sum (\rho_0 - \hat{\rho}_0) \sum_t \sum_{a_t} P_p(\cdot|s_t, a_t) \gamma^t r_p(s_t, a_t) \right| \\ &\leq \bar{r} \left| \sum (\rho_0 - \hat{\rho}_0) \sum_t \sum_{a_t} P_p(\cdot|s_t, a_t) \gamma^t \right| \\ &\leq \bar{r} \left| \sum (\rho_0 - \hat{\rho}_0) \sum_t \gamma^t \right| \\ &\leq \frac{\bar{r}}{1-\gamma} \sum |\rho_0 - \hat{\rho}_0| = \frac{2\bar{r}}{1-\gamma} D_{\text{TV}}(\rho_0, \hat{\rho}_0). \end{aligned}$$

For  $L_2$ , we have

$$\begin{aligned} L_2 &= \left| \mathbb{E}_{\hat{\rho}_0} \mathbb{E}_{P_p} \left[ \sum_{t=0}^{\infty} \gamma^t r_p(s_t, a_t) \right] - \mathbb{E}_{\hat{\rho}_0} \mathbb{E}_{\hat{P}_p} \left[ \sum_{t=0}^{\infty} \gamma^t r_p(s_t, a_t) \right] \right| \\ &= \left| \sum \hat{\rho}_0 \sum_t \sum_{a_t} (P_p(\cdot|s_t, a_t) - \hat{P}_p(\cdot|s_t, a_t)) \gamma^t r_p(s_t, a_t) \right|. \end{aligned}$$

If the accumulated uncertainty is large, i.e.,  $T_t^\epsilon = 1$ , then  $P_p(\cdot|s, a) = \hat{P}_p(\cdot|s, a) = 0$ . Otherwise, we have  $P_p(\cdot|s, a) = P(\cdot|s, a)$  and  $\hat{P}_p(\cdot|s, a) = \hat{P}(\cdot|s, a)$ , respectively. We denote the termination horizon as  $T$ . In the  $\epsilon$ -Pessimistic MDP, we require that  $\sum_{t=0}^T \gamma^t D_{\text{TV}}(P(\cdot|s_t, a_t), \hat{P}(\cdot|s_t, a_t)) \leq \epsilon$ . Then it holds that for any horizon  $i \leq T, i \in \mathbb{Z}$ , we have  $|\sum_{t=0}^i \sum_{a_t} \gamma^t (P(\cdot|s_t, a_t) - \hat{P}(\cdot|s_t, a_t))| \leq \epsilon$  almost surely. Therefore, we have

$$\begin{aligned} L_2 &= \left| \sum \hat{\rho}_0 \sum_t \sum_{a_t} (P_p(\cdot|s_t, a_t) - \hat{P}_p(\cdot|s_t, a_t)) \gamma^t r_p(s_t, a_t) \right| \\ &\leq \bar{r} \left| \sum \hat{\rho}_0 \sum_t \sum_{a_t} (P_p(\cdot|s_t, a_t) - \hat{P}_p(\cdot|s_t, a_t)) \gamma^t \right| \\ &\leq \bar{r} \cdot \epsilon \cdot \left| \sum \hat{\rho}_0 \right| = \bar{r} \cdot \epsilon. \end{aligned}$$

By combining the upper bounds of  $L_1$  and  $L_2$ , we have the desired result immediately.  $\square$

We also have the following lemma:

**Lemma 2.** *Set  $\bar{r} = r_{\max} + \lambda u_{\max} + \kappa$ . Given the pessimistic MDP  $\mathcal{M}_p$  and the true MDP  $\mathcal{M}$ , the return difference of any policy  $\pi$  on the two MDPs is bounded:*

$$\begin{aligned} J_{\rho_0}(\pi, \mathcal{M}_p) &\geq J_{\rho_0}(\pi, \mathcal{M}) - \frac{\bar{r}}{1-\gamma}, \\ J_{\rho_0}(\pi, \mathcal{M}_p) &\leq J_{\rho_0}(\pi, \mathcal{M}). \end{aligned} \quad (13)$$

*Proof.* For the first part, we have

$$\begin{aligned} & J_{\rho_0}(\pi, \mathcal{M}_p) - J_{\rho_0}(\pi, \mathcal{M}) \\ &= \sum \rho_0 \sum_t \sum_{a_t} \gamma^t (P_p(\cdot|s_t, a_t) r_p(s_t, a_t) - P(\cdot|s_t, a_t) r(s_t, a_t)) \\ &= \sum \rho_0 \sum_t \sum_{a_t} \gamma^t (P_p(\cdot|s_t, a_t) (r_p(s_t, a_t) - r(s_t, a_t))) \\ &\quad + \sum \rho_0 \sum_t \sum_{a_t} \gamma^t ((P_p(\cdot|s_t, a_t) - P(\cdot|s_t, a_t)) r(s_t, a_t)). \end{aligned}$$

Furthermore, we have  $r_p(s, a) - r(s, a) \geq -(\lambda u_{\max} + \kappa)$  as  $0 \leq u(s, a) \leq u_{\max}, \forall s, a$ . We also notice that  $P_p(\cdot|s, a) = 0$  if the trajectory is truncated at  $(s, a)$ , and  $P_p(\cdot|s, a) = P(\cdot|s, a)$  otherwise. Hence,  $P_p(\cdot|s, a) - P(\cdot|s, a) \leq 0$ . Then we have,

$$\begin{aligned} & J_{\rho_0}(\pi, \mathcal{M}_p) - J_{\rho_0}(\pi, \mathcal{M}) \\ &\geq -(\lambda u_{\max} + \kappa) \sum \rho_0 \sum_t \sum_{a_t} \gamma^t P_p(\cdot|s_t, a_t) \\ &\quad - r_{\max} \sum \rho_0 \sum_t \sum_{a_t} \gamma^t P(\cdot|s_t, a_t)) = -\frac{\bar{r}}{1-\gamma}. \end{aligned}$$

For the second part, using the definition of the reward function in the pessimistic MDP, the rewards obtained by any policy  $\pi$  on each transition in  $\mathcal{M}_p$  is less than the reward obtained in  $\mathcal{M}$ . Therefore, the second part holds, which concludes the proof.  $\square$

We then can formally prove Theorem 1, which is restated below.

**Theorem 2.** Denote  $\bar{r} = r_{\max} + \lambda u_{\max} + \kappa$ . Then the return of any policy  $\pi$  in the  $\epsilon$ -Pessimistic MDP  $\hat{\mathcal{M}}_p$  and its original MDP  $\mathcal{M}$  satisfies:

$$\begin{aligned} J_{\hat{\rho}_0}(\pi, \hat{\mathcal{M}}_p) &\geq J_{\rho_0}(\pi, \mathcal{M}) - \frac{2\bar{r}}{1-\gamma} \cdot D_{\text{TV}}(\rho_0, \hat{\rho}_0) \\ &\quad - \bar{r} \cdot \epsilon - \frac{\bar{r}}{1-\gamma}, \end{aligned} \quad (14)$$

$$\begin{aligned} J_{\hat{\rho}_0}(\pi, \hat{\mathcal{M}}_p) &\leq J_{\rho_0}(\pi, \mathcal{M}) + \frac{2\bar{r}}{1-\gamma} \cdot D_{\text{TV}}(\rho_0, \hat{\rho}_0) \\ &\quad + \bar{r} \cdot \epsilon. \end{aligned} \quad (15)$$

*Proof.* We decompose  $J_{\hat{\rho}_0}(\pi, \hat{\mathcal{M}}_p) - J_{\rho_0}(\pi, \mathcal{M})$  as:

$$\underbrace{J_{\hat{\rho}_0}(\pi, \hat{\mathcal{M}}_p) - J_{\rho_0}(\pi, \mathcal{M}_p)}_{(I)} + \underbrace{J_{\rho_0}(\pi, \mathcal{M}_p) - J_{\rho_0}(\pi, \mathcal{M})}_{(II)}.$$

Then by bounding term (I) with Lemma 1 and bounding term (II) using Lemma 2, we can conclude the proof.  $\square$

## A.2 Proof of Corollary 1 and 2

We restate the Corollary 1 below.

**Corollary 3.** If the policy in the  $\epsilon$ -Pessimistic MDP is  $\epsilon_\pi$  sub-optimal, i.e.,  $J_{\hat{\rho}_0}(\pi, \hat{\mathcal{M}}_p) \geq J_{\hat{\rho}_0}(\pi^*, \hat{\mathcal{M}}_p) - \epsilon_\pi$ , then we have

$$\begin{aligned} J_{\rho_0}(\pi^*, \mathcal{M}) - J_{\rho_0}(\pi, \mathcal{M}) &\leq \epsilon_\pi + \frac{4\bar{r}}{1-\gamma} \cdot D_{\text{TV}}(\rho_0, \hat{\rho}_0) \\ &\quad + 2\bar{r}\epsilon + \frac{\bar{r}}{1-\gamma}. \end{aligned}$$

*Proof.* By using the results in Theorem 1 and the assumption on the sub-optimality, we have

$$\begin{aligned} J_{\rho_0}(\pi, \mathcal{M}) &\geq J_{\hat{\rho}_0}(\pi, \hat{\mathcal{M}}_p) - \frac{2\bar{r}}{1-\gamma} D_{\text{TV}}(\rho_0, \hat{\rho}_0) - \bar{r}\epsilon \\ &\geq J_{\hat{\rho}_0}(\pi^*, \hat{\mathcal{M}}_p) - \epsilon_\pi - \frac{2\bar{r}}{1-\gamma} D_{\text{TV}}(\rho_0, \hat{\rho}_0) - \bar{r}\epsilon \\ &\geq J_{\rho_0}(\pi^*, \mathcal{M}) - \epsilon_\pi - \frac{4\bar{r}}{1-\gamma} D_{\text{TV}}(\rho_0, \hat{\rho}_0) - 2\bar{r}\epsilon \\ &\quad - \frac{\bar{r}}{1-\gamma}. \end{aligned}$$

This concludes the proof.  $\square$

If the dataset is large enough, then all of the generated transitions will be in-distribution and hence admitted. Then  $D_{\text{TV}}(\rho_0, \hat{\rho}_0)$  and  $\epsilon$  approach 0. By setting  $D_{\text{TV}}(\rho_0, \hat{\rho}_0) = 0$  and  $\epsilon = 0$  in Corollary 1 conclude the proof of Corollary 2.

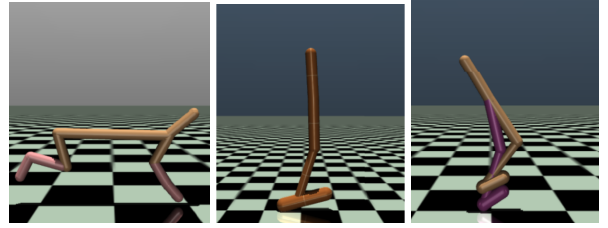


Figure 2: MuJoCo datasets from D4RL. From left to right, halfcheetah, hopper, walker2d.

## B Experimental Setup and Hyperparameter Setup

In this section, we present the detailed experimental setup for TATU. We introduce the datasets we adopted in this paper and provide a detailed hyperparameter setup we used for all of the base algorithms and our TATU.

### B.1 MuJoCo Datasets on the D4RL Benchmark

In our evaluation, we utilize three tasks from the MuJoCo dataset, halfcheetah, hopper, and walker2d as illustrated in Figure 2. Each task contains five types of datasets: (1) **random** where samples are collected by a random policy; (2) **medium** where the samples are collected from an early-stopped SAC policy for 1M steps; (3) **medium-replay** where samples are gathered using the replay buffer of a policy that trained up to the medium-level agent; (4) **medium-expert** where samples are collected by mixing the medium-level data and expert-level data at a 50-50 ratio; (5) **expert** where the dataset is logged with an expert policy.

The normalized score is widely used for evaluating the performance of the agent on the offline dataset. Denote the expected return of a random policy as  $J_{\text{random}}$ , and the expected return of an expert policy as  $J_{\text{expert}}$ . Assume the return obtained by the policy  $\pi$  gives  $J_\pi$ , then the normalized score (NS) gives:

$$NS = \frac{J_\pi - J_{\text{random}}}{J_{\text{expert}} - J_{\text{random}}} \times 100. \quad (16)$$

It can be seen that the normalized score generally ranges from 0 to 100, where 0 corresponds to a random policy and 100 corresponds to an expert policy. The reference scores for the random policy and expert policy are previously set by D4RL.

### B.2 Implementation Details

**TATU implementation details.** In our experiments, we train the forward dynamics model with a neural network parameterized by  $\psi$  to output a multivariate Gaussian distribution for predicting the next state,

$$\hat{p}_\psi(s'|s, a) = \mathcal{N}(\mu_\theta(s, a), \Sigma_\phi(s, a)), \psi = \{\theta, \phi\},$$

where  $\mu_\theta(s, a)$  and  $\Sigma_\phi(s, a)$  denote the mean and variance of the forward model, respectively. As mentioned in the main text, we model the difference in the current state and the next state to ensure local continuity. We model the probabilistic neural network with a multi-layer neural network that consists of 4 feedforward layers with 200 hidden units. Each intermediate layer in the network adopts swish activation. We train

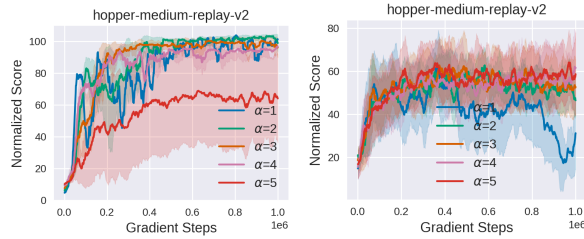


Figure 3: Normalized average score comparison of TATU+MOPO and TATU+TD3\_BC on hopper-medium-replay-v2 under different threshold coefficients  $\alpha$ . The results are averaged over 5 different random seeds and the shaded region is the standard deviation.

an ensemble of seven such neural networks by following prior work [Janner *et al.*, 2019]. We use a validation set of 1000 transitions to validate the performance of the learned dynamics models. When generating imaginations, we first select the best five models out of seven candidates and then randomly pick one from them for imagined trajectory generation. For other parameters that are not quite relevant to TATU (e.g., hyperparameters of the base algorithms), we simply follow their default setting. We then give more experimental details on the key parameters in TATU as shown below:

**Reward penalty coefficient  $\lambda$ .**  $\lambda$  determines how large penalty we add to the generated samples, since the pessimistic reward function in the  $\epsilon$ -Pessimistic MDP gives  $r_p(s, a) = r(s, a) - \lambda u(s_t, a_t)$ . Larger  $\lambda$  will inject more conservatism into the imagined samples. Considering the fact that there are many other important hyperparameters in TATU (e.g., threshold coefficient  $\alpha$ , real data ratio  $\eta$ , etc.), we choose to fix this parameter. To be specific, we set  $\lambda = 1.0$  on all of the evaluated tasks. One may possibly get better results by carefully tuning this parameter, and one can also refer to the suggested  $\lambda$  adopted in the MOPO’s official codebase (<https://github.com/tianheyu927/mopo>).

**Threshold coefficient  $\alpha$ .** The threshold coefficient  $\alpha$  is one of the most important hyperparameters for TATU under different datasets and tasks. Note that the uncertainty threshold  $\epsilon = \frac{1}{\alpha} \max_{i \in \{1, \dots, |\mathcal{D}|\}} u(s_i, a_i)$ .  $\alpha$  thus controls how tolerable we are to the imagined trajectory. Larger  $\alpha$  indicates that only very conservative trajectories that lie in the span of the dataset can be trusted, and smaller  $\alpha$  will admit more trajectories. Generally, we set  $\alpha \geq 1$  such that the accumulated uncertainty along the imagined trajectory will not exceed the maximum uncertainty in the real dataset, which ensures the reliability of the samples in the model buffer  $\mathcal{D}_{\text{model}}$ . Empirically, we find that setting  $\alpha = 2$  can incur very satisfying performance on most of the evaluated datasets. Some exceptions are hopper-medium-v2, hopper-medium-expert-v2, and hopper-expert-v2 where  $\alpha = 3.5$  is set to involve more pessimistic samples. We further present in Figure 3 the learning curves comparison of TATU+MOPO and TATU+TD3\_BC on hopper-medium-replay-v2 dataset under  $\alpha \in \{1.0, 2.0, 3.0, 4.0, 5.0\}$ .

**Rollout horizon  $h$ .** The rollout horizon decides how far can the synthetic trajectory branch from the starting state. Intuitively, a larger rollout horizon  $h$  may involve more di-

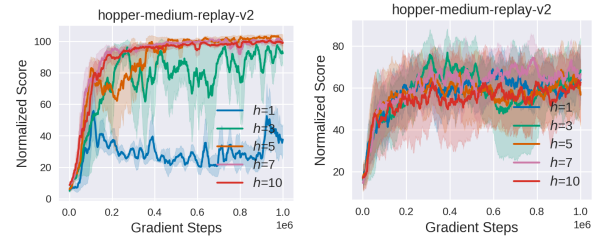


Figure 4: Performance of TATU+MOPO and TATU+TD3\_BC with different rollout horizons on hopper-medium-replay-v2. The results are averaged over 5 different random seeds, and we report the mean performance and the standard deviation.

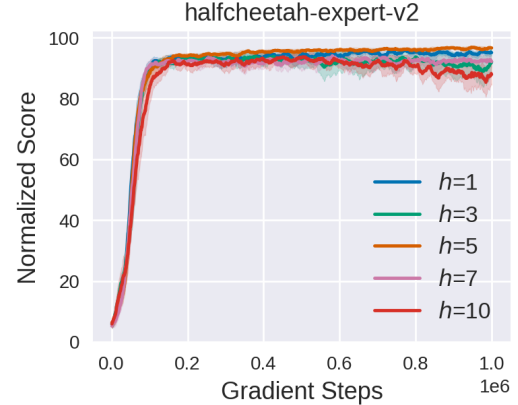


Figure 5: Performance of TATU+TD3\_BC on halfcheetah-expert-v2 with different  $h$ . The results are averaged over 5 runs. We report the mean performance and the standard deviation here.

verse transition data (as the trajectory is longer). In our main experiments, we set rollout horizon  $h = 5$  for all the datasets from MuJoCo, i.e., halfcheetah, hopper, and walker2d. In the main text, we conduct a parameter study on  $h$  in Section 5.3, where only final performance is reported. Here, we give the learning curves of TATU+MOPO and TATU+TD3\_BC on hopper-medium-replay-v2 in Figure 4, where we use  $h \in \{1, 3, 5, 7, 10\}$ . Furthermore, we conduct additional experiments using TATU+TD3\_BC on halfcheetah-expert-v2. The results are shown in Figure 5. We find that TATU+TD3\_BC prefers a smaller horizon  $h = 1$  while it seems a larger horizon is better for TATU+MOPO and TATU+TD3\_BC on hopper-medium-replay-v2. This is due to the fact that generated samples are more likely to be OOD on expert datasets (with narrow span). On the medium-replay dataset, a longer horizon can still ensure that the imaginations are in-distribution and hence the base algorithms can benefit from more conservative imaginations (i.e., better generalization ability).

**Real data ratio  $\eta$ .** When updating the offline policy, we sample a mini-batch (of size  $B$ ) from  $\mathcal{D} \cup \mathcal{D}_{\text{model}}$ . Then we sample  $\eta B$  samples from the real dataset  $\mathcal{D}$  and  $(1 - \eta)B$  samples from the model buffer  $\mathcal{D}_{\text{model}}$  given the real data ratio  $\eta \in [0, 1]$ . When combining TATU with model-based offline RL methods, we follow their original parameter setup for

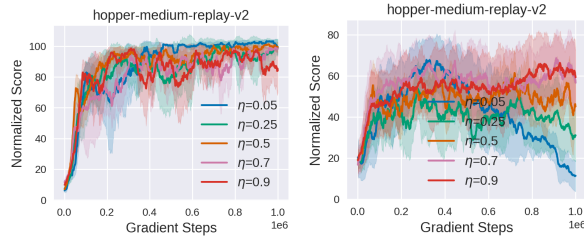


Figure 6: Performance of TATU+MOPO and TATU+TD3<sub>BC</sub> on hopper-medium-replay-v2 using different real data ratios. All methods are run for 5 different random seeds, and the shaded region captures the standard deviation.

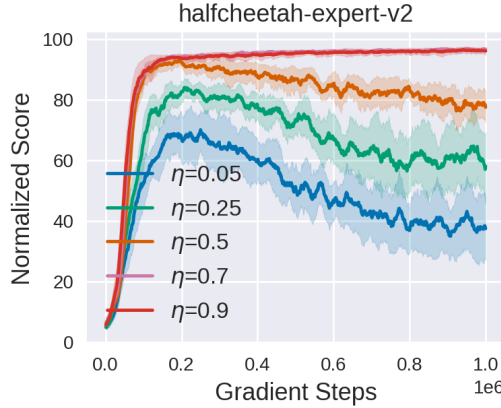


Figure 7: Performance of TATU+TD3<sub>BC</sub> on halfcheetah-expert-v2 with different  $\eta$ . The results are averaged over 5 runs and the shaded area denotes the standard deviation.

real data ratio, i.e.,  $\eta = 0.05$  for TATU+MOPO and  $\eta = 0.5$  for TATU+COMBO across all the datasets. As for the combination with model-free offline RL,  $\eta$  strongly depends on the type of the dataset, i.e., small  $\eta$  is better for datasets with poor quality while larger  $\eta$  is preferred for datasets with high quality (e.g., expert datasets). We provide the detailed parameter setting for  $\eta$  in Table 7. For most of the datasets, we use  $\eta = 0.7$  or  $\eta = 0.9$  which we find can ensure a quite satisfying performance. We show in Figure 6 the learning curves of TATU+MOPO and TATU+TD3<sub>BC</sub> under different real data ratios  $\eta \in \{0.05, 0.25, 0.5, 0.7, 0.9\}$ . We further illustrate in Figure 7 the performance of TATU+TD3<sub>BC</sub> on halfcheetah-expert-v2 under different real data ratios. The result is consistent with our analysis above.

## C Compute Infrastructure

We list our compute infrastructure below.

- Python: 3.7.13
- Pytorch: 1.12.0+cu113
- Gym: 0.24.1
- MuJoCo: 2.3.0
- D4RL: 1.1
- TensorFlow: 2.10.0

Table 7: Real data ratio  $\eta$  adopted in TATU when combined with model-free offline RL algorithms. r = random, m = medium, m-r = medium-replay, m-e = medium-expert, e = expert. All experiments are run on D4RL MuJoCo ‘‘v2’’ datasets.

Task Name	TATU+TD3 <sub>BC</sub>	TATU+CQL	TATU+BCQ
half-r	0.7	0.7	0.7
hopper-r	0.1	0.7	0.7
walker2d-r	0.1	0.7	0.7
half-m-r	0.5	0.9	0.9
hopper-m-r	0.7	0.7	0.7
walker2d-m-r	0.5	0.9	0.9
half-m	0.7	0.9	0.9
hopper-m	0.9	0.9	0.9
walker2d-m	0.7	0.9	0.9
half-m-e	0.7	0.9	0.9
hopper-m-e	0.9	0.9	0.9
walker2d-m-e	0.7	0.9	0.9
half-e	0.7	0.9	0.9
hopper-e	0.9	0.9	0.9
walker2d-e	0.7	0.9	0.9

- GPU: RTX3090 ( $\times 8$ )
- CPU: AMD EPYC 7452

## D Full Experimental Comparison

Please refer to Table 8 and 9 the full experimental comparison of TATU against baseline methods when combined with model-based offline RL algorithms and model-free offline RL algorithms, respectively.

Table 8: Normalized average score comparison of TATU+MOPPO and TATU+COMBO against their base algorithms and some recent baselines on the D4RL MuJoCo “-v2” dataset. half = halfcheetah, r = random, m = medium, m-r = medium-replay, m-e = medium-expert. Each algorithm is run for 1M gradient steps with 5 different random seeds. We report the final performance.  $\pm$  captures the standard deviation. We bold the top 2 score of the left part and the best score of the right part.

Task Name	TATU+MOPPO	MOPPO	TATU+COMBO	COMBO	BC	CQL	IQL	DT	MOReL
half-r	33.3 $\pm$ 2.6	<b>35.9</b> $\pm$ 2.9	29.3 $\pm$ 2.7	<b>38.8</b> $\pm$ 3.7	2.2 $\pm$ 0.0	17.5 $\pm$ 1.5	13.1 $\pm$ 1.3	-	<b>38.9</b> $\pm$ 1.8
hopper-r	<b>31.3</b> $\pm$ 0.6	16.7 $\pm$ 12.2	<b>31.6</b> $\pm$ 0.6	17.9 $\pm$ 1.4	3.7 $\pm$ 0.6	7.9 $\pm$ 0.4	7.9 $\pm$ 0.2	-	<b>38.1</b> $\pm$ 10.1
walker2d-r	<b>10.4</b> $\pm$ 0.7	4.2 $\pm$ 5.7	5.3 $\pm$ 0.0	<b>7.0</b> $\pm$ 3.6	1.3 $\pm$ 0.1	5.1 $\pm$ 1.3	5.4 $\pm$ 1.2	-	<b>16.0</b> $\pm$ 7.7
half-m-r	<b>67.2</b> $\pm$ 3.3	<b>69.2</b> $\pm$ 1.1	57.8 $\pm$ 2.7	55.1 $\pm$ 1.0	37.6 $\pm$ 2.1	<b>45.5</b> $\pm$ 0.7	44.2 $\pm$ 1.2	36.6 $\pm$ 0.8	44.5 $\pm$ 5.6
hopper-m-r	<b>104.4</b> $\pm$ 0.9	32.7 $\pm$ 9.4	<b>100.7</b> $\pm$ 1.3	89.5 $\pm$ 1.8	16.6 $\pm$ 4.8	88.7 $\pm$ 12.9	<b>94.7</b> $\pm$ 8.6	82.7 $\pm$ 7.0	81.8 $\pm$ 17.0
walker2d-m-r	<b>75.3</b> $\pm$ 0.2	73.7 $\pm$ 9.4	<b>75.3</b> $\pm$ 1.7	56.0 $\pm$ 8.6	20.3 $\pm$ 9.8	<b>81.8</b> $\pm$ 2.7	73.8 $\pm$ 7.1	66.6 $\pm$ 3.0	40.8 $\pm$ 20.4
half-m	61.9 $\pm$ 2.9	<b>73.1</b> $\pm$ 2.4	<b>69.2</b> $\pm$ 2.8	54.2 $\pm$ 1.5	43.2 $\pm$ 0.6	47.0 $\pm$ 0.5	47.4 $\pm$ 0.2	42.6 $\pm$ 0.1	<b>60.7</b> $\pm$ 4.4
hopper-m	<b>104.3</b> $\pm$ 1.3	38.3 $\pm$ 34.9	<b>100.0</b> $\pm$ 1.3	97.2 $\pm$ 2.2	54.1 $\pm$ 3.8	53.0 $\pm$ 28.5	66.2 $\pm$ 5.7	67.6 $\pm$ 1.0	<b>84.0</b> $\pm$ 17.0
walker2d-m	<b>77.9</b> $\pm$ 1.6	41.2 $\pm$ 30.8	77.4 $\pm$ 0.9	<b>81.9</b> $\pm$ 2.8	70.9 $\pm$ 11.0	73.3 $\pm$ 17.7	<b>78.3</b> $\pm$ 8.7	74.0 $\pm$ 1.4	72.8 $\pm$ 11.9
half-m-e	74.1 $\pm$ 1.4	70.3 $\pm$ 21.9	<b>96.4</b> $\pm$ 3.6	<b>90.0</b> $\pm$ 5.6	44.0 $\pm$ 1.6	75.6 $\pm$ 25.7	86.7 $\pm$ 5.3	<b>86.8</b> $\pm$ 1.3	80.4 $\pm$ 11.7
hopper-m-e	<b>107.0</b> $\pm$ 1.3	60.6 $\pm$ 32.5	106.5 $\pm$ 0.4	<b>111.1</b> $\pm$ 2.9	53.9 $\pm$ 4.7	105.6 $\pm$ 12.9	91.5 $\pm$ 14.3	<b>107.6</b> $\pm$ 1.8	105.6 $\pm$ 8.2
walker2d-m-e	<b>107.9</b> $\pm$ 0.9	77.4 $\pm$ 27.9	<b>114.6</b> $\pm$ 0.7	103.3 $\pm$ 5.6	90.1 $\pm$ 13.2	107.9 $\pm$ 1.6	<b>109.6</b> $\pm$ 1.0	108.1 $\pm$ 0.2	107.5 $\pm$ 5.6
Average score	<b>71.3</b>	49.4	<b>72.0</b>	66.8	36.5	59.1	59.9	-	<b>64.3</b>

Table 9: Normalized average score comparison of TATU+TD3\_BC, TATU+CQL and TATU+BCQ against their base algorithms and some recent baselines on the D4RL MuJoCo “-v2” dataset. half = halfcheetah, r = random, m = medium, m-r = medium-replay, m-e = medium-expert, e = expert. Each algorithm is run for 1M gradient steps across 5 different random seeds and the final mean performance is reported.  $\pm$  captures the standard deviation. We bold the top 3 score of the left part and the best score of the right part.

Task Name	TATU+TD3_BC	TD3_BC	TATU+CQL	CQL	TATU+BCQ	BCQ	BC	IQL	DT
half-r	<b>12.1</b> $\pm$ 2.3	11.0 $\pm$ 1.1	<b>27.4</b> $\pm$ 2.6	<b>17.5</b> $\pm$ 1.5	2.3 $\pm$ 2.3	2.2 $\pm$ 0.0	2.2 $\pm$ 0.0	<b>13.1</b> $\pm$ 1.3	-
hopper-r	<b>31.6</b> $\pm$ 0.6	8.5 $\pm$ 0.6	<b>32.3</b> $\pm$ 0.7	7.9 $\pm$ 0.4	<b>10.3</b> $\pm$ 0.8	7.8 $\pm$ 0.6	3.7 $\pm$ 0.6	<b>7.9</b> $\pm$ 0.2	-
walker2d-r	<b>21.4</b> $\pm$ 0.0	1.6 $\pm$ 1.7	<b>23.0</b> $\pm$ 0.0	<b>5.1</b> $\pm$ 1.3	3.4 $\pm$ 0.4	4.9 $\pm$ 0.1	1.3 $\pm$ 0.1	<b>5.4</b> $\pm$ 1.2	-
half-m-r	<b>45.9</b> $\pm$ 0.6	44.6 $\pm$ 0.5	<b>48.0</b> $\pm$ 0.7	<b>45.5</b> $\pm$ 0.7	43.5 $\pm$ 0.3	42.2 $\pm$ 0.9	37.6 $\pm$ 2.1	<b>44.2</b> $\pm$ 1.2	36.6 $\pm$ 0.8
hopper-m-r	65.7 $\pm$ 3.9	60.9 $\pm$ 18.8	<b>96.8</b> $\pm$ 2.6	<b>88.7</b> $\pm$ 12.9	<b>72.9</b> $\pm$ 0.4	60.9 $\pm$ 14.7	16.6 $\pm$ 4.8	<b>94.7</b> $\pm$ 8.6	82.7 $\pm$ 7.0
walker2d-m-r	81.9 $\pm$ 2.7	81.8 $\pm$ 5.5	<b>85.5</b> $\pm$ 1.2	<b>81.8</b> $\pm$ 2.7	77.7 $\pm$ 1.0	57.0 $\pm$ 9.6	20.3 $\pm$ 9.8	<b>73.8</b> $\pm$ 7.1	66.6 $\pm$ 3.0
half-m	<b>48.4</b> $\pm$ 2.7	<b>48.3</b> $\pm$ 0.3	44.9 $\pm$ 0.3	47.0 $\pm$ 0.5	<b>47.6</b> $\pm$ 0.2	46.6 $\pm$ 0.4	43.2 $\pm$ 0.6	<b>47.4</b> $\pm$ 0.2	42.6 $\pm$ 0.1
hopper-m	<b>62.0</b> $\pm$ 1.0	59.3 $\pm$ 4.2	<b>68.9</b> $\pm$ 0.9	53.0 $\pm$ 28.5	<b>71.0</b> $\pm$ 0.3	59.4 $\pm$ 8.3	54.1 $\pm$ 3.8	66.2 $\pm$ 5.7	<b>67.6</b> $\pm$ 1.0
walker2d-m	<b>84.3</b> $\pm$ 0.2	<b>83.7</b> $\pm$ 2.1	65.7 $\pm$ 0.5	73.3 $\pm$ 17.7	<b>80.5</b> $\pm$ 0.4	71.8 $\pm$ 7.2	70.9 $\pm$ 11.0	<b>78.3</b> $\pm$ 8.7	74.0 $\pm$ 1.4
half-m-e	<b>97.1</b> $\pm$ 3.2	90.7 $\pm$ 4.3	78.9 $\pm$ 0.5	75.6 $\pm$ 25.7	<b>96.1</b> $\pm$ 0.2	<b>95.4</b> $\pm$ 2.0	44.0 $\pm$ 1.6	86.7 $\pm$ 5.3	<b>86.8</b> $\pm$ 1.3
hopper-m-e	<b>113.0</b> $\pm$ 1.7	98.0 $\pm$ 9.4	<b>111.5</b> $\pm$ 1.0	105.6 $\pm$ 12.9	<b>108.2</b> $\pm$ 0.3	106.9 $\pm$ 5.0	53.9 $\pm$ 4.7	91.5 $\pm$ 14.3	<b>107.6</b> $\pm$ 1.8
walker2d-m-e	<b>110.9</b> $\pm$ 0.5	110.1 $\pm$ 0.5	<b>110.2</b> $\pm$ 0.1	107.9 $\pm$ 1.6	<b>111.7</b> $\pm$ 0.3	107.7 $\pm$ 3.8	90.1 $\pm$ 13.2	<b>109.6</b> $\pm$ 1.0	108.1 $\pm$ 0.2
half-e	<b>97.4</b> $\pm$ 0.4	<b>96.7</b> $\pm$ 1.1	90.8 $\pm$ 3.4	<b>96.3</b> $\pm$ 1.3	<b>96.3</b> $\pm$ 1.4	89.9 $\pm$ 9.6	91.8 $\pm$ 1.5	<b>95.0</b> $\pm$ 0.5	-
hopper-e	111.8 $\pm$ 1.1	<b>107.8</b> $\pm$ 7	106.8 $\pm$ 0.9	96.5 $\pm$ 28.0	103.9 $\pm$ 0.6	<b>109.0</b> $\pm$ 4.0	107.7 $\pm$ 0.7	<b>109.4</b> $\pm$ 0.5	-
walker2d-e	<b>110.0</b> $\pm$ 0.1	<b>110.2</b> $\pm$ 0.3	108.3 $\pm$ 0.1	108.5 $\pm$ 0.5	<b>109.7</b> $\pm$ 0.3	106.3 $\pm$ 5.0	106.7 $\pm$ 0.2	<b>109.9</b> $\pm$ 1.2	-
Average score	<b>72.9</b>	67.5	<b>73.3</b>	67.3	<b>69.0</b>	64.5	49.6	<b>68.9</b>	-